Spatial Proteomics and Epigenomics Reveal Cell Morphology and Epigenetic Gene Regulation in Human Hippocampus

Yang Xiao[1,2]#, Graham Su[3,4]#, Yuqi Tan[5]#, Nima Asaad[6,7], Yanxiang Deng[3,8], Tianyu Li[1], Yao Lu[3], Dongjoo Kim[3], Gorazd B. Rosoklija[9,10,11], Archibald Enninful[3,4], Zhiliang Bai[3,4], Yang Liu[3], Cheick Sissoko[9,10], Madeline Mariani[9,10], Tingting Wu[12], Phi Nguyen[9,13], Huiyi Liang[1], Adrienne Santiago[9,13], Andrew J. Dwork[9,10,11,14], René Hen[9,13,15,16], Garry P. Nolan[5,17], J. John Mann[9,10,18], Sai Ma[6,7], Kam W. Leong[1,2]*, and Maura Boldrini[9,10]*, and Rong Fan[3,4,19,20]*

Supplementary Documents (6 Figures, 2 Tables, 1 Movie)

S. Figure 1. Quality control metrics for a representative spatial mRNA-seq dataset.

S. Figure 2. Regional annotation in each sample.

S. Figure 3. Cell type deconvolution through integration of single nucleus transcriptomes and spatial transcriptomes.

S. Figure 4. Cell type deconvolution of inhibitory neuron subtypes (CTRL_04).

S. Figure 5. Region-specific RNA velocity.

S. Figure 6. Spatial chromatin accessibility profiling in the dentate gyrus of the hippocampus.

S.Table 1_CODEX cell_counts_per_sample.csv

S.Table 2_List of PCR Oligo and DNA Barcode Sequences.xlsx

S.Movie 1_CTRL01_Spatial_Proteome.mov

A

	CTRL_1	CTRL_2	CTRL_3	CTRL_4	CTRL_5	CTRL_6	MDD_1	MDD_3	MDD_4	MDD_5
Raw Reads	278,998,676	255,590,786	126,838,892	203,456,136	316,836,560	316,142,378	213,608,210	126,994,400	133,192,618	354,545,956
Ratio of reads with L1 with L2	0.675849657	0.790173615	0.785533188	0.491253215	0.803420233	0.785294982	0.716502895	0.770638887	0.734636625	0.777066888
Uniquely mapped reads STP	22,315,987	20,319,840	5,078,690	8,540,759	25,290,691	13,654,950	7,024,318	14,292,567	24,717,444	18,417,256
Total Unique UMIs	4,550,895	3,988,458	1,335,918	3,692,729	4,892,724	1,789,317	1,350,663	5,178,463	3,908,152	1,920,893
Total Gene Count	2,359,192	1,943,445	1,009,374	2,348,589	2,357,175	980,380	967,466	2,837,807	2,385,562	1,096,736
Number of Unique Genes Present	23,669	22,858	19,318	22,369	24,113	20,161	20,376	22,925	25,744	21,783
Average UMIs per pixel	1,820	1,595	534	1,477	1,957	716	540	2,071	1,563	768
Max UMI per pixel	11,811	18,900	4,940	32,863	16,428	4,838	15,841	16,656	24,555	10,833
Standard Deviation of UMIs per pixel	1,770	1,765	665	1,542	2,045	534	944	2,065	2,318	927
Average Gene Count per pixel	944	777	403	939	943	392	387	1,135	954	439
Max Gene Count per pixel	4,299	5,047	2,767	6,285	5,111	2,285	5,937	5,287	7,030	4,356
Standard Deviation of Gene Count per pixel	722	630	431	680	810	296	511	813	979	469

B

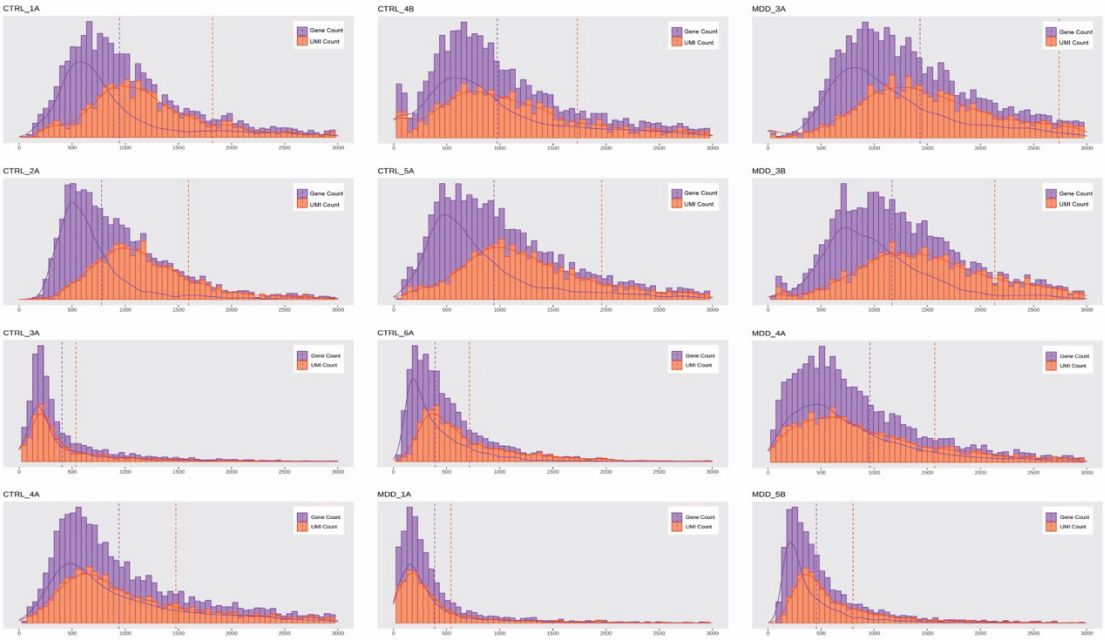

Supplementary Figure 1. Quality control metrics for a representative spatial mRNA-seq dataset.
(A) Quantitative metrics assessing mRNA sequencing quality.
(B) Frequency distributions of the gene counts (purple) and unique molecular index (UMI) counts (orange).

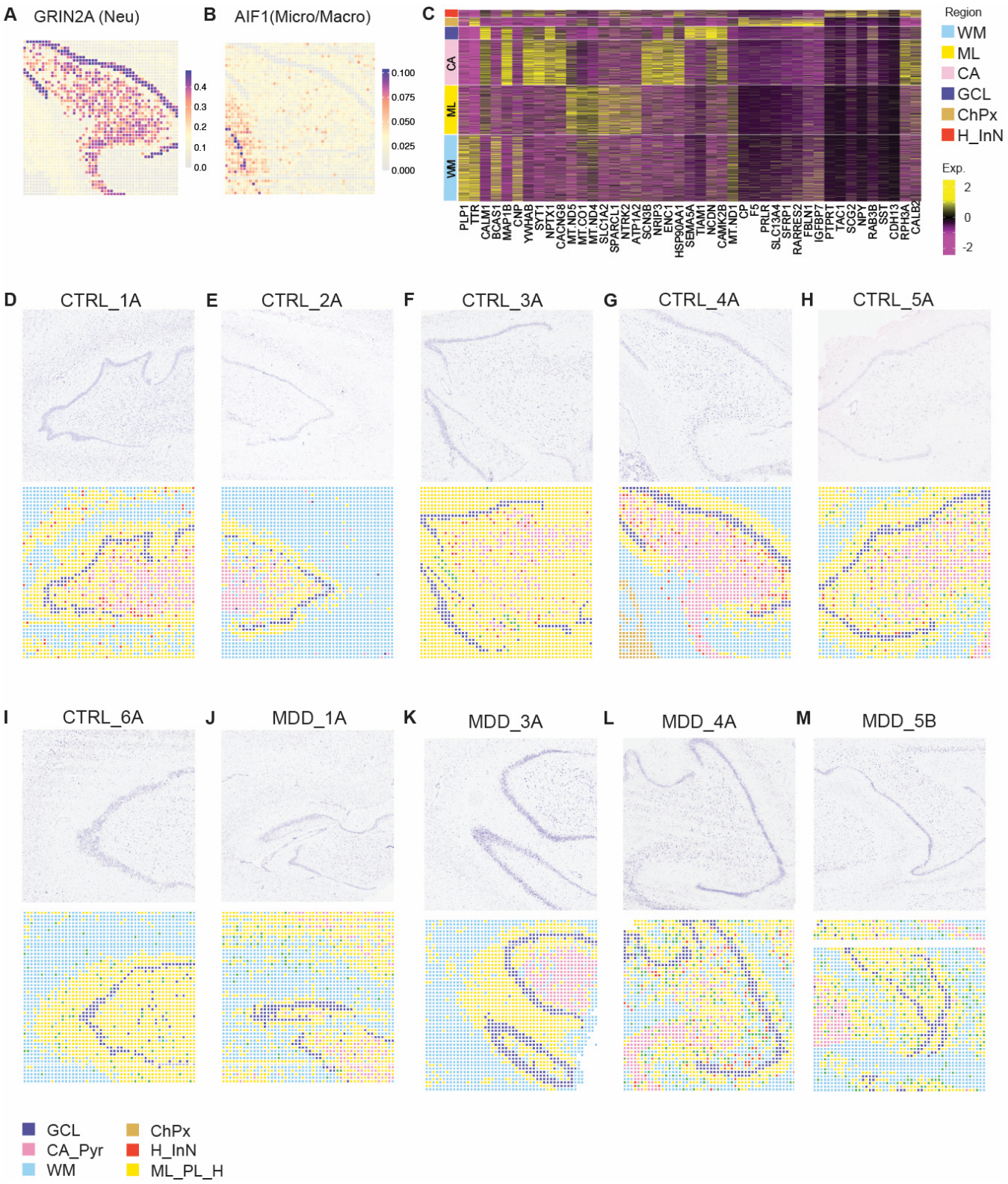

Supplementary Figure 2. Regional annotation in each sample.

(**A-B**) Spatial maps of key cell type-specific gene expression. *Neu*: neuron; *Micro/Macro*: microglia or

macrophages.

(**C**) The heatmap of signature gene expression identified through unsupervised clustering. *GCL*: Granule Cell Layer; *CA_Pyr*: pyramidal neurons in the cornu Ammonis; *WM*: white matter; *ML_PL_H*: molecular layer, polymorphic layer, and hilus; *ChPx*: choroid plexus; *H_InN*: inhibitory neurons in the hilus region.

(**D-M**) Annotated anatomical subfields of the hippocampus. The first row of each subpanel shows a Nissl-stained adjacent slice. The second row displays the hippocampal subfields identified via unsupervised clustering, with each color representing a distinct cluster. *GCL*: Granule Cell Layer; *CA_Pyr*: pyramidal neurons in the cornu Ammonis; *WM*: white matter; *ML_PL_H*: molecular layer, polymorphic layer, and hilus; *ChPx*: choroid plexus; *H_InN*: inhibitory neurons in the hilus region.

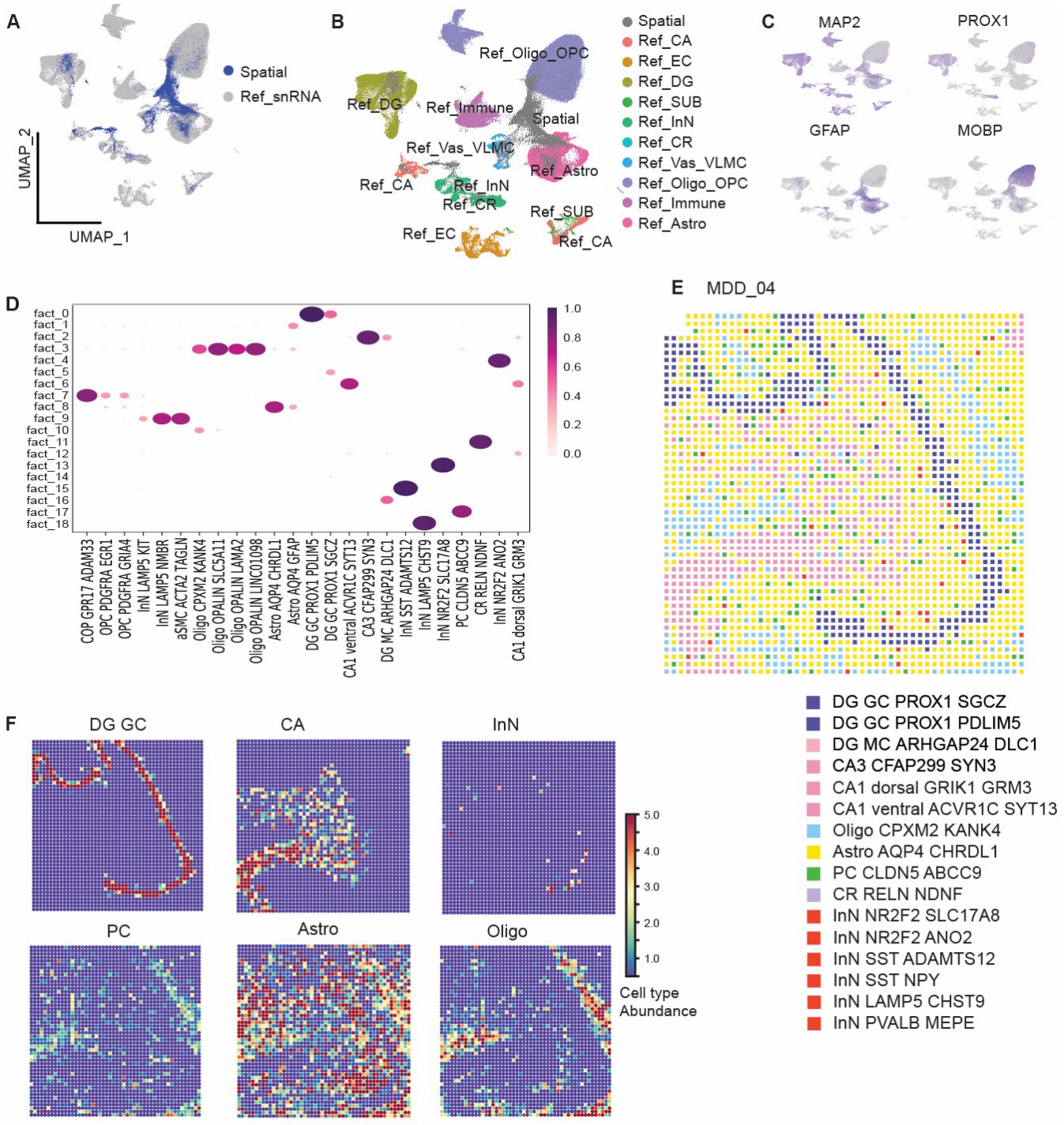

Supplementary Figure 3. Cell type deconvolution through integration of single nucleus transcriptomes and spatial transcriptomes.

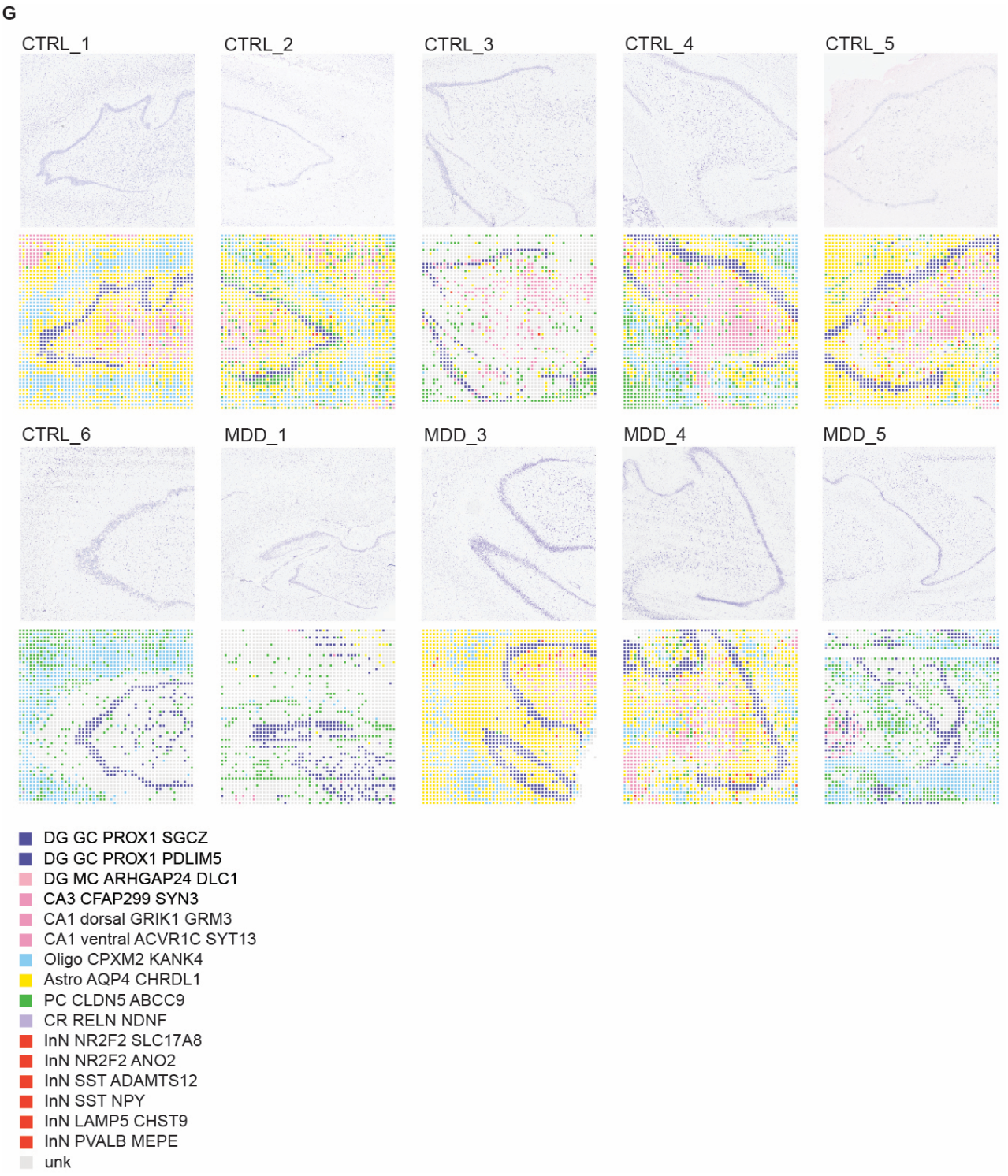

Supplementary Figure 3 (Continued). Cell type deconvolution through integration of single nucleus transcriptomes and spatial transcriptomes.

(**A**) UMAP visualization of unsupervised clustering of spatial data and reference snRNA-seq data, color by dataset origin.

(**B**) UMAP representation of the single-cell and spatial dataset with cells color-coded based on their cell types.

(**C**) Key marker genes in neurons (MAP2), granule neurons (PROX1), astrocytes (GFAP), and oligodendrocytes (MOBP).

(**D**) Factorization of the cell subtype abundance scores across all spatial spots. Each row represents a distinct spatial pattern of cell distribution. Subtypes of oligodendrocytes co-localize, as shown in Factor 3. In contrast, subtypes of inhibitory neurons display mutually exclusive spatial distributions, represented by Factor 4,13, 15, and 18.

(**E**) Integrative analysis with snRNA-seq data inference the cell types in MDD_04 brain. Spatial maps of the most abundant cell type were shown in each spot, statistically computed by Cell2location algorithm.

(**F**) Predicted maps of cell abundance by cell2location algorithm. Each subpanel represents a cell type in the reference snRNA-seq.

(**G**) Spatial maps of the most abundant cell type in each sample, predicted by cell2location algorithm.

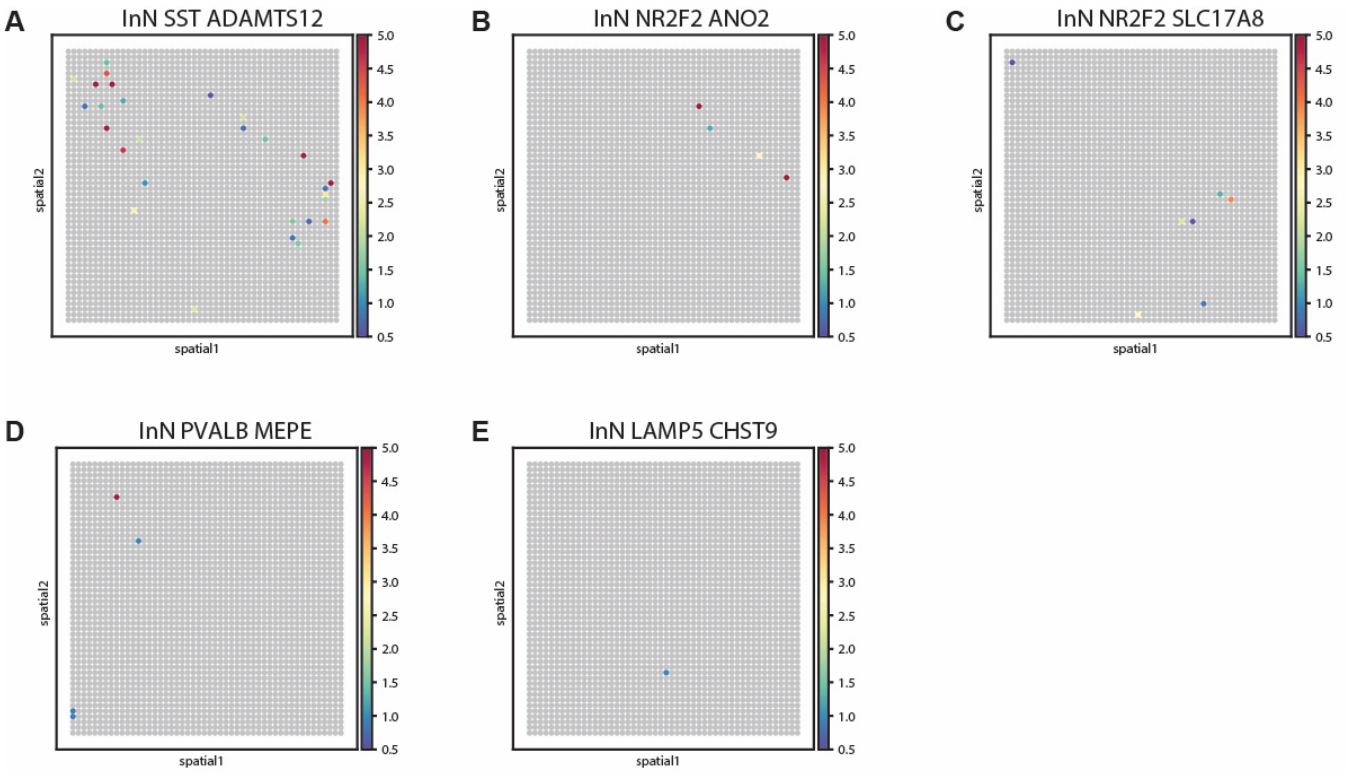

Supplementary Figure 4. Cell type deconvolution of inhibitory neuron subtypes (CTRL_04)

(A) The predicted map of “InN SST ADAMTS12” cell abundance by cell2location algorithm.

(B) The predicted map of “InN NR2F2 ANO2” cell abundance by cell2location algorithm.

(C) The predicted map of “InN NR2F2 SLC17A8” cell abundance by cell2location algorithm.

(D) The predicted map of “InN PVALB MEPE” cell abundance by cell2location algorithm.

(E) The predicted map of “InN LAMP5 CHST9” cell abundance by cell2location algorithm.

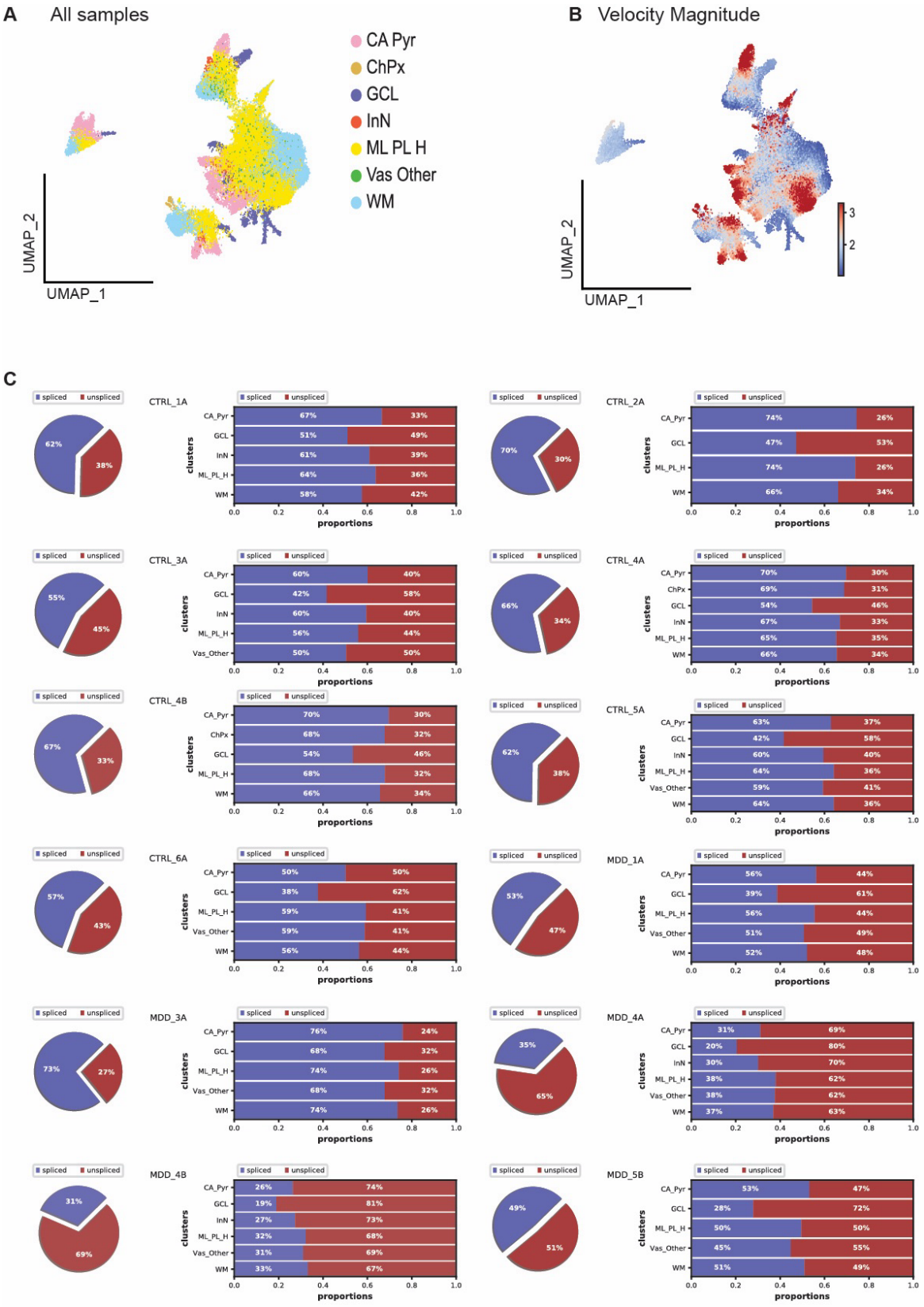

Supplementary Figure 5. Spatial RNA velocity reveals region-specific cell dynamics.

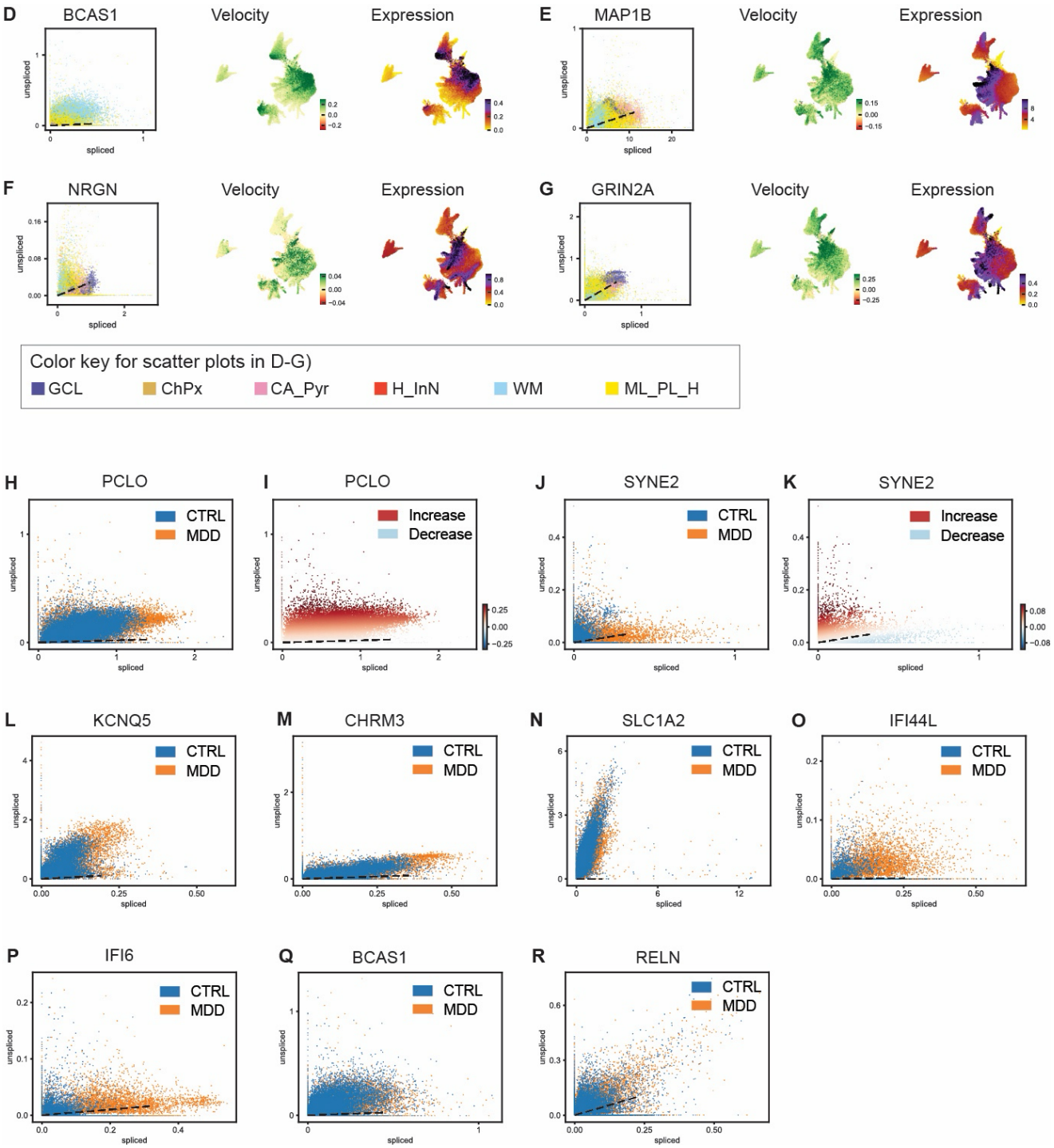

Supplementary Figure 5 (Continued). Spatial RNA velocity reveals region-specific cell dynamics. (**A**) Unsupervised clustering based on both spliced and unspliced mRNAs across all samples, colored by anatomical regions. A total of 2,500 pixels were collected per sample, resulting in 37,240 spatial pixels from six control and six MDD samples. *GCL*: Granule Cell Layer; *CA_Pyr*: pyramidal neurons in the cornu Ammonis; *WM*: white matter; *ML_PL_H*: molecular layer, polymorphic layer, and hilus; *ChPx*: choroid plexus; *InN*: inhibitory neurons in the hilus region.

(**B**) Unsupervised clustering based on both spliced and unspliced mRNAs across all samples, colored by RNA velocity magnitude.

(C) The proportions of spliced and unspliced mRNAs in each human brain (pie charts). Bar plots show the proportions of spliced and unspliced mRNAs in each anatomical layer. Spliced counts are shown in purple, while unspliced counts are shown in dark red.

(D-G) The phase portraits of specific genes: D) BCAS1; E) MAP1B; F) NGRN; G) GRIN2A. Each point corresponds to a spatial pixel, colored by anatomical region. “velocity” is the computed RNA velocity rate, indicating whether this gene is increasing or decreasing in expression. “expression” is the measured gene expression level.

(H, J, L-R) The phase portraits of the spliced/unspliced mRNA across all samples. Each point corresponded to a spatial pixel, colored by disease group (CTRL: Blue; MDD: Orange). Steady states fell on the dashed line.

(**I, K**) Levels of unspliced mRNA above or below the dashed line indicated increasing (red dots) or decreasing (blue dots) gene expression.

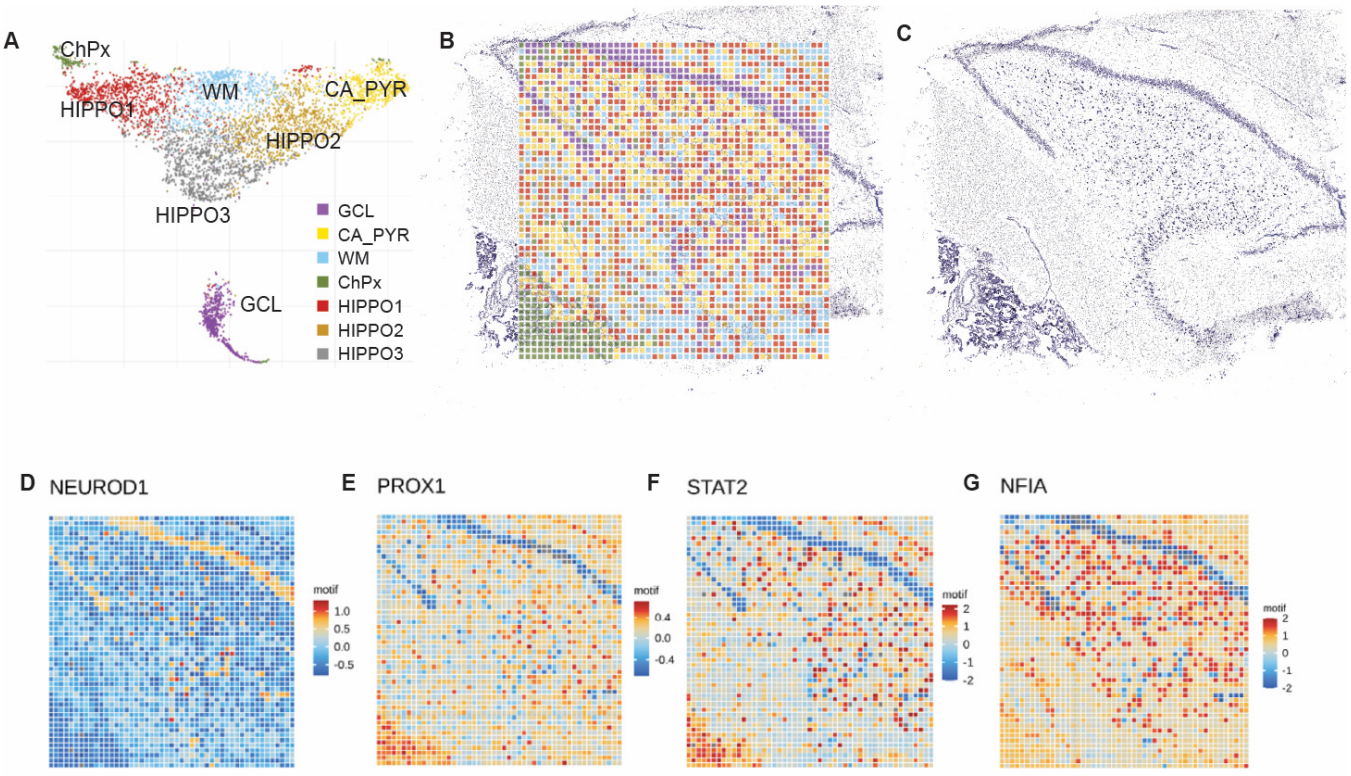

Supplementary Figure 6. Spatial chromatin accessibility profiling in the dentate gyrus of the hippocampus (CTRL_04).

(A) UMAP visualization of unsupervised clustering of the spatial ATAC-seq data. Each dot represents a sequencing library collected from one 50 x 50 μm^2 spatial pixel. There are 2,500 dots in the UMAP. *GCL*: Granule Cell Layer; *CA_Pyr*: pyramidal neurons in the cornu Ammonis; *WM*: white matter; *ChPx*: choroid plexus; HIPPO1,HIPPO2, HOPPO3: hippocampus regions identified based on open chromatin, no correlated anatomical subfield is assigned.

(B) Spatial map of the clusters in (A).

(**C**) A Nissl-stained adjacent slice showing the geometry of the mid-hippocampus region.

(D-G) Motif scores for the spatially most variable transcription factors in GCL of CTRL_04 sample.